Chapter 7

Model-Independent Trilepton Search

Events containing three or more leptons are useful probes of phenomena beyond the Standard Model. The production of three or more leptons is predicted by many models of phenomena beyond the Standard Model, as described in section 2.2. The expected Standard Model backgrounds are typically small; depending on the flavor and charge of the three leptons, such events primarily arise from diboson production (WZ, ZZ), or from single boson (W, Z/γ^*) or $t\bar{t}$ production along with one or more leptons from misidentified or semileptonically decaying jets. This dissertation presents two such searches: a model-independent search for nonresonant production of three or more leptons in many signal regions, and a signature-driven search for resonance trilepton production in the context of heavy leptons.

This chapter presents a search for physics beyond the Standard Model using events containing three or more leptons [1]. The search uses 20.3 fb^{-1} of pp collision data taken at $\sqrt{s} = 8$ TeV with the ATLAS detector. Many signal regions are defined based on the properties of the leptons, jets, and overall momentum imbalance of the event, with the goal of being broadly sensitive to the nonresonant production of trilepton final states by phenomena beyond the Standard Model. The results are first presented in a model-independent fashion, establishing upper limits on the production of events with three or more charged leptons from non-Standard Model sources. The limits are then used to confront a model predicting new doubly charged scalar particles.

7.1 Event Selection

This section describes the selection of events containing at least three leptons in the pp collision data and Monte Carlo simulation samples.

7.1.1 Triggering

Collisions events for this analysis are triggered using the unprescaled single-electron or single-muon triggers with the lowest transverse momentum thresholds. At least one of the following

triggers must have fired:

- `EF_e24vhi_medium1`: One electron with $p_{\mathrm{T}} > 24$ GeV. The electron must satisfy cuts similar to the `medium++` identification criteria at the trigger level, an isolation requirement of $\frac{p_{\mathrm{T}}^{\mathrm{cone20}}}{p_{\mathrm{T}}} < 0.1$, and cuts on the leakage into the hadronic calorimeter.
- `EF_e60_medium1`: One electron with $p_{\mathrm{T}} > 60$ GeV. The electron must also satisfy the medium identification cuts, but the isolation and leakage requirements are removed.
- `EF_mu24i_tight`: One muon with $p_{\mathrm{T}} > 24$ GeV, satisfying an isolation requirement of $\frac{p_{\mathrm{T}}^{\mathrm{cone20}}}{p_{\mathrm{T}}} < 0.12$.
- `EF_mu36_tight`: One muon with $p_{\mathrm{T}} > 36$ GeV, with no isolation requirement.

The triggers with higher tranverse momentum thresholds remove the isolation requirements in order to improve the efficiency at higher p_{T}. Triggered events are required to have an offline lepton matched to the trigger object within $\Delta R = \sqrt{(\Delta\eta)^2 + (\Delta\phi)^2} < 0.1$. To avoid trigger turn-on effects near the p_{T} threshold, the offline lepton must have $p_{\mathrm{T}} > 26$ GeV. Additionally, trigger-matched muons must have $|\eta| < 2.4$ to avoid uninstrumented regions of the detector.

7.1.2 Trilepton Event Selection

After successful triggering and overlap removal, events are required to have at least three selected leptons, with at most one hadronically decaying tau lepton. The primary event vertex, chosen as the reconstructed vertex with the highest $\sum p_{\mathrm{T}}^2$ of tracks, must have at least three tracks. Finally, events are rejected if they contain "bad jets" not associated to real energy deposits in the calorimeters due to pp collisions, i.e. from electronics problems or cosmic rays [2].

7.2 Analysis Strategy

The analysis defines a large number of nonexclusive signal regions, designed to target new physics models and to compartmentalize the expected backgrounds. First, the events are divided into six categories as follows. First, the events are divided into three categories based on the properties of any opposite-sign, same-flavor (OSSF) lepton pairs in the event:

- **on-Z**: events containing an OSSF lepton pair consistent with the decay of a Z boson, with invariant mass within 20 GeV of m_Z;
- **off-Z, OSSF**: events containing an OSSF pair that do not fall in the on-Z category; and

- **off-Z, mixed**: events containing no OSSF pairs.

The on-Z category also includes events containing three leptons (two of which form an OSSF pair) with invariant mass within 20 GeV of m_Z, to include events containing a Z boson where a photon from final state radiation converts and is reconstructed as a prompt electron.

Next, the events are further divided into two categories based on the number of electron or muon candidates in the event:

- **3L**: events containing at least three electrons or muons, and
- **2L**+τ_{had}: events containing exactly two electrons or muons and a hadronically decaying tau lepton.

After dividing the events into these six exclusive categories, many signal regions are defined based on the lower bound in various kinematic variables. An ordering is imposed on the leptons for the sake of disambiguation: in the 3L category, the leptons are ordered by p_{T}, while in the 2L category, the electrons or muons are ordered by p_{T}, and the τ_{had} is the third lepton. The variables used to define the signal regions are:

- $H_{\text{T}}^{\text{leptons}}$: the scalar sum of the transverse momenta of the leading three leptons. Events containing new particles with masses significantly greater than m_W or m_Z will typically have larger $H_{\text{T}}^{\text{leptons}}$ than the Standard Model backgrounds.
- Minimum p_{T}^{ℓ}: the p_{T} of the softest of the leading three leptons. As with $H_{\text{T}}^{\text{leptons}}$, the p_{T} of leptons produced in the decays of heavy particles will tend to be larger than those from the expected Standard Model backgrounds.
- $H_{\text{T}}^{\text{jets}}$: the scalar sum of the transverse momenta of all selected jets in the event. This variable is sensitive to the strongly produced new physics, where leptons are produced in the decays of heavy colored particles, such as squarks. Such events often contain hard jets in addition to the three leptons. Conversely, the Standard Model WZ and ZZ backgrounds are weakly produced, and have softer $H_{\text{T}}^{\text{jets}}$ distributions.
- $E_{\text{T}}^{\text{miss}}$: the magnitude of the missing transverse momentum in the event. In models of new physics, leptons can be produced in association with new invisible particles, such as stable neutralinos in R-parity conserving supersymmetry, or with neutrinos in leptonic W decays. Requiring large $E_{\text{T}}^{\text{miss}}$ can distinguish such signals from the Standard Model backgrounds, where the $E_{\text{T}}^{\text{miss}}$ is primarily due to neutrinos from W or τ decays. Requiring large $E_{\text{T}}^{\text{miss}}$ also suppresses backgrounds due to Z+jets, where the jet decays semileptonically or is misidentified as a lepton.
- m_{eff}: the scalar sum of $H_{\text{T}}^{\text{jets}}$, $E_{\text{T}}^{\text{miss}}$, and the p_{T} of all identified leptons in the event. As with $H_{\text{T}}^{\text{leptons}}$ by itself, multilepton production due to the decays of heavy particles will typically have a harder m_{eff} distribution than the Standard Model backgrounds.

Variable	Meaning
$H_{\mathrm{T}}^{\mathrm{jets}}$	Σp_{T} of all jets in the event
m_{T}^{W}	Transverse mass of W-boson candidate (on-Z events only)

Variable	Meaning	Lower Bounds [GeV]				Additional Requirements
$H_{\mathrm{T}}^{\mathrm{leptons}}$	Σp_{T} of leading three leptons	0	200	500	800	
Min. p_{T}^{ℓ}	p_{T} of softest (third) lepton	0	50	100	150	
$E_{\mathrm{T}}^{\mathrm{miss}}$	Missing transverse momentum	0	100	200	300	$H_{\mathrm{T}}^{\mathrm{jets}} < 150$ GeV
$E_{\mathrm{T}}^{\mathrm{miss}}$		0	100	200	300	$H_{\mathrm{T}}^{\mathrm{jets}} \geq 150$ GeV
m_{eff}		0	600	1000	1500	
m_{eff}	All transverse activity	0	600	1200		$E_{\mathrm{T}}^{\mathrm{miss}} \geq 100$ GeV
m_{eff}		0	600	1200		$m_{\mathrm{T}}^{W} \geq 100$ GeV, on-Z

Variable	Meaning	Lower Bounds	
b-tags	Number of b-tagged jets	1	2

Table 7.1: Kinematic signal regions defined in the analysis.

- m_{T}^{W}: for events in the on-Z categories, the transverse mass of the missing transverse momentum, $\vec{p}_{\mathrm{T}}^{\mathrm{miss}}$, and the highest-$p_{\mathrm{T}}$ lepton not associated with a Z boson candidate, defined as:
$$m_{\mathrm{T}}^{W} = \sqrt{2|\vec{p}_{\mathrm{T}}^{\ell}||\vec{p}_{\mathrm{T}}^{\mathrm{miss}}|(1-\cos(\Delta\phi))}, \tag{7.1}$$
where $\Delta\phi$ is the azimuthal angle between the transverse momentum of the lepton, $\vec{p}_{\mathrm{T}}^{\ell}$, and the missing transverse momentum, $\vec{p}_{\mathrm{T}}^{\mathrm{miss}}$.

- $N_{b-\mathrm{tags}}$, the number of b-tagged jets. New physics scenarios related to the hierarchy problem (section 2.2) often couple preferentially to the third generation, due to the dominant effect of the top quark in the running of the Higgs mass.

The signal regions are defined in table 7.1. The signal regions use one of $H_{\mathrm{T}}^{\mathrm{leptons}}$, the minimum p_{T}^{ℓ}, $E_{\mathrm{T}}^{\mathrm{miss}}$, m_{eff}, and n_b as binning variables. $H_{\mathrm{T}}^{\mathrm{jets}}$, $E_{\mathrm{T}}^{\mathrm{miss}}$, and m_{T}^{W} are used to impose additional requirements on the signal regions. In total, 138 signal regions are defined.

7.3 Systematic Uncertainties

Systematic uncertainties are assigned to the signal and background predictions to account for possible modelling inaccuracies. The sources of uncertainty considered are:

- Uncertainties on the reducible background estimates from the data-driven estimation method, as described in section 6.2.1. The uncertainties ranges between 20% to 30% for the electron fake factors, 25% to 50% for the muon fake factors, and 25% to 30% for the tau lepton fake factors.

Sample	Uncertainty
$t\bar{t}+V$	30% [3, 4]
ZZ	4.3%
WZ	7.6%

Table 7.2: Systematic uncertainties used for the MC samples that contribute to the background estimates.

- Simulated Monte Carlo samples, whether signal or background, must be normalized to the integrated luminosity of the data. The weight assigned to each event is:

$$w = \frac{\mathcal{L}\sigma_{\text{process}}}{N_{\text{sim}}}, \tag{7.2}$$

  where $\mathcal{L}$ is the integrated luminosity of the data, σ_{process} is the cross section of the simulated process, and N_{sim} is the number of simulated events. The integrated luminosity carries an uncertainty of 2.8%, as described in section 4.5. The cross sections are taken from calculations with uncertainties due to various sources, including the fixed order of the calculation, the choice of renormalization and factorization scales, and the PDFs. For the dominant WZ and ZZ backgrounds, the predictions from SHERPA are compared to those from the next-to-leading-order generator VBFNLO. The generators show good agreement, and the systematic uncertainty on the cross section is determined from VBFNLO by varying the factorization and renormalization scales up and down by factors of two. The uncertainties are shown in table 7.2.

  No systematic uncertainty is assigned to the normalization of the $Z+\gamma$ sample. Rather, a large uncertainty of 30% is assigned due to the reweighting procedure described in section 10.1.1. The $VVV^{(*)}$ sample is also not assigned an uncertainty due to its small contribution to the signal regions.

- Events are also weighted to account for differences between data and Monte Carlo simulation in the lepton trigger, reconstruction, and identification efficiencies. The scale factors and associated uncertainties are provided by the relevant ATLAS combined performance groups. The electron (section 5.2.2) and muon (section 5.3.1) scale factors are close to unity, with uncertainties in the range 1-5%. The scale factors for the tau lepton identification efficiency range from 94-96% for the `BDTTight` working point, and carry uncertainties between 2.0-2.2% (section 5.4).

- The lepton energy scales carry uncertainty which has a small effect on the signal regions due to leptons or events near E_{T} or p_{T} thresholds, as described in sections 5.2.3, 5.3.2, and 5.4.1.

- The jet energies are scaled and smeared according to recommendations from the `JetEtMiss` combined performance group (section 5.5.1). The uncertainty affects the $H_{\mathrm{T}}^{\mathrm{jets}}$ and m_{eff} distributions, and also the lepton-jet overlap removal procedure.
- The lepton and jet energy uncertainties are also propagated to the missing transverse energy, $E_{\mathrm{T}}^{\mathrm{miss}}$.
- The efficiencies of the b-tagging algorithm carry uncertainties which are parameterized based on matching the identified b-jets to truth b-jets.
- Finally, the Monte Carlo samples carry statistical uncertainty due to simulating a finite number of events.

The dominant sources of uncertainty depend on the signal region, but are generally due to Monte Carlo statistical uncertainties, the fake factor uncertainites, and theoretical cross section uncertainties.

7.4 Background Validation

The background estimates are verified in several dedicated validation regions, which are orthogonal to the signal regions. Events containing two leptons are used to test the selection of prompt leptons and their corresponding scale factors and energy corrections. The reducible backgrounds are tested in $t\bar{t}$ validation regions, where the events are required to have two same-sign leptons to target semileptonic decays where one lepton arises from a reducible process. Finally, the fake factor method is validated in events with modified, intermediate lepton selections, where the signal leptons are between the numerator and denominator definitions used in the nominal reducible background estimate.

7.4.1 Dilepton Validation Regions

Three dilepton validation regions target the three flavors of leptons: ee, $\mu\mu$, and $\mu\tau_{\mathrm{had}}$. The ee and $\mu\mu$ regions require an opposite-sign lepton pair of the appropriate flavor. The invariant mass distributions of the dilepton system in these regions are shown in figure 7.1. Some disagreement is observed in the ee invariant mass distribution; this discrepancy is covered by the electron energy scale systematic uncertainties.

The ee and $\mu\mu$ validation regions are also used to generate scale factors to account for efficiency differences between simulation and data when applying cuts on lepton isolation or impact parameter. The scale factors are computed from events with a dilepton pair with invariant mass within 10 GeV of m_Z, and are shown in figure 7.2. The scale factors are mostly consistent with unity to within 0.5%, except for isolation requirements on the low-p_{T} leptons, where the scale factors deviate from unity by up to 2%.

The $\mu\tau_{\mathrm{had}}$ region applies addition cuts to reduce the large contribution from fake tau leptons in W+jets events:

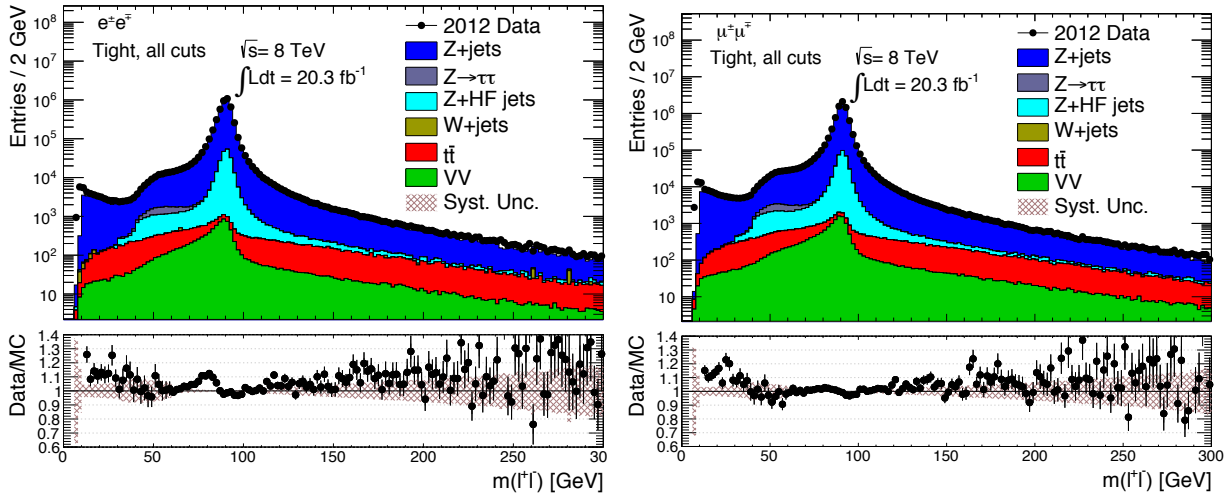

(a) ee (b) $\mu\mu$

Figure 7.1: Dilepton invariant mass distributions for the ee (left) and $\mu\mu$ (right) validation regions.

- $\cos\Delta\phi(\mu, E_{\mathrm{T}}^{\mathrm{miss}}) + \cos\Delta\phi(\tau, E_{\mathrm{T}}^{\mathrm{miss}}) > -0.15$,
- $\Delta\phi(\mu, \tau_{had}) > 2.4$,
- $m_{\mathrm{T}}^{\mu} < 50$ GeV,
- $42 < m_Z^{vis.} < 82$ GeV, and
- $p_{\mathrm{T}}^{\mu} < 40$ GeV.

The p_{T} distribution of the $\tau_{\text{had-vis}}$ is shown in figure 7.3.

7.4.2 $t\bar{t}$ Validation Regions

In signal regions that veto Z bosons and require large $H_{\mathrm{T}}^{\mathrm{jets}}$ or $E_{\mathrm{T}}^{\mathrm{miss}}$, a large reducible background component is expected from $t\bar{t}$ events, where both W bosons decay leptonically and a third lepton arises from a misidentified jet or semileptonic heavy flavor decay. This process is tested in the $t\bar{t}$ validation regions, which require at least one b-tagged jet with $p_{\mathrm{T}} >$ 30 GeV, exactly two electrons or muons with the same charge, and $H_{\mathrm{T}}^{\mathrm{jets}} < 500$ GeV. The requirement that the leptons have the same sign vetoes dilepton $t\bar{t}$ events with two prompt leptons from W decays, while the $H_{\mathrm{T}}^{\mathrm{jets}}$ requirement reduces the potential contamination from new BSM phenomena. Note that events containing hadronically decaying tau leptons are used to derive a systematic uncertainty on the tau fake factors due to the flavor composition of the events (section 6.2.4), and so are not used as a validation region.

The $E_{\mathrm{T}}^{\mathrm{miss}}$ distribution of events in the $t\bar{t}$ validation region is shown in figure 7.4.

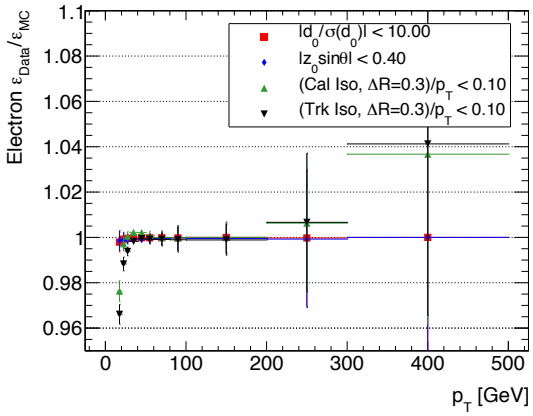

(a) Electron p_{T} Scale Factors

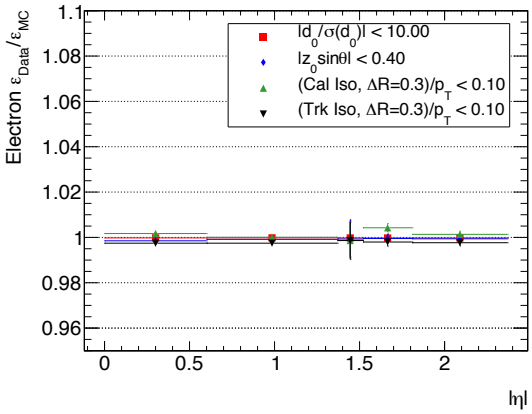

(b) Electron $|\eta|$ Scale Factors

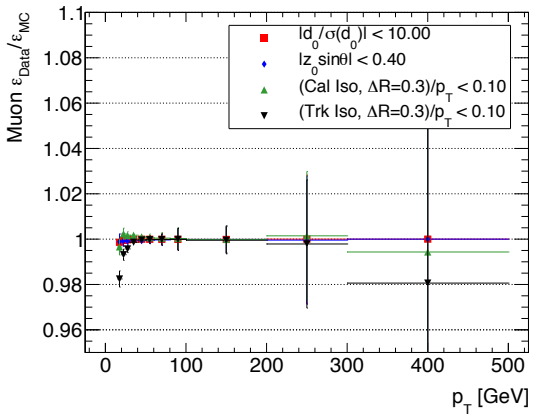

(c) Muon p_{T} Scale Factors

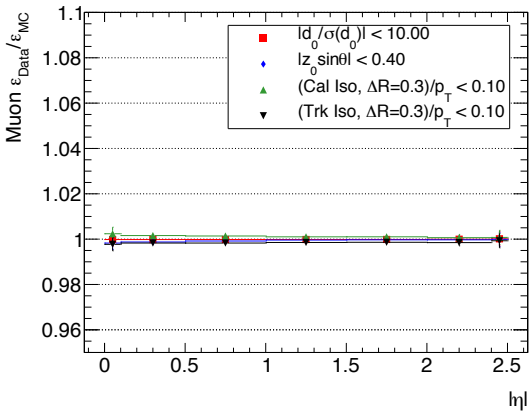

(d) Muon $|\eta|$ Scale Factors

Figure 7.2: Scale factors for electrons and muons as functions of p_{T} (left) and $|\eta|$ (right).

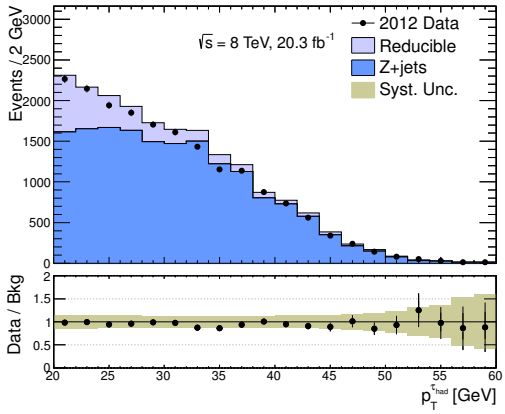

Figure 7.3: p_{T} distribution of the $\tau_{\text{had-vis}}$ candidates in the $\mu\tau_{\text{had}}$ validation region.

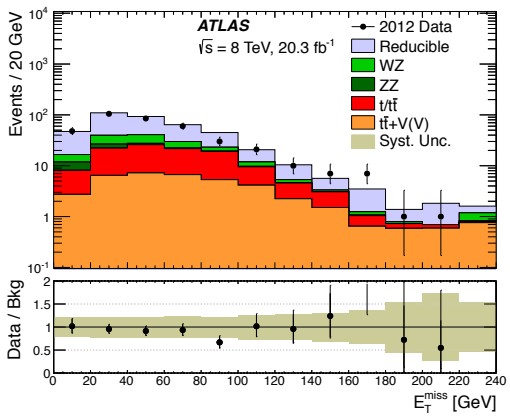

Figure 7.4: $t\bar{t}$ validation regions for all flavor (e, μ) combinations.

7.4.3 Intermediate Fake Factor Validation Regions

The fake factor method is further validated in regions containing events with two signal (numerator) leptons and one "intermediate" lepton, which fulfills selection criteria looser than the numerator criteria but tighter than the denominator criteria. Separate fake factors are derived for intermediate leptons; these are defined schematically as ⟨intermediate⟩/⟨denominator⟩, rather than ⟨numerator⟩/⟨denominator⟩. Specifically, the intermediate leptons satisfy most of the numerator criteria except for:

- **Electrons**: the electron must pass the `medium++` cuts, but fail the `tight++` cuts.
- **Muons**: the candidate must have either its track or calorimeter transverse isolation energy satisfy $0.10 < \text{iso}/p_{\text{T}} < 0.15$.
- **Taus**: the tau candidate must pass the `Medium-BDT` identification requirement, but fail the `tight-BDT` identification requirement.

The first two regions, targeting reducible electrons and muons, require an OSSF pair of electrons or muons, plus a third intermediate electron or muon of the opposite flavor. The events are largely due to $Z \to ee$ or $Z \to \mu\mu$ events, with an additional lepton that is either prompt and fails the signal lepton criteria, or is due to a reducible process. The p_{T} and η distributions of the intermediate electrons and muons are shown in figure 7.5.

The events containing an intermediate τ_{had} are much more abundant than intermediate electrons or muons, so three τ_{had} validation regions are defined, mirroring the signal region categories. Events are required to contain two electrons or muons plus an intermediate τ_{had}, and are separated into on-Z, off-Z/OSSF, and off-Z/mixed categories, depending on the two electrons or muons. The p_{T} and η of the intermediate τ_{had} is shown for each category in figure 7.6.

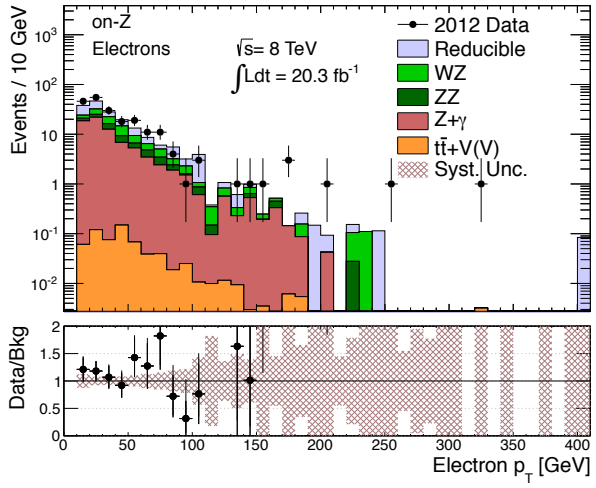

(a) Intermediate electron p_{T}

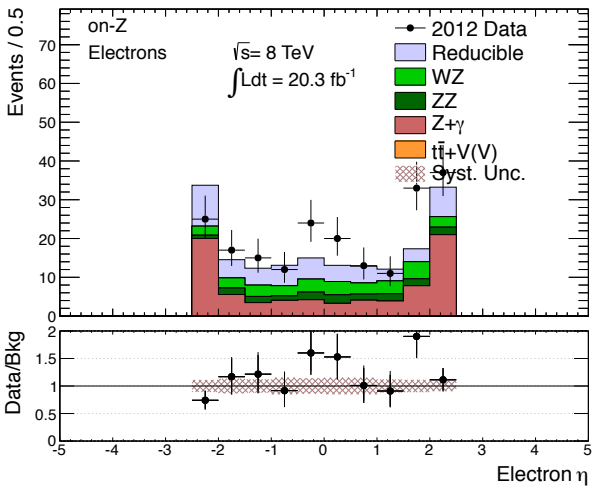

(b) Intermediate electron η

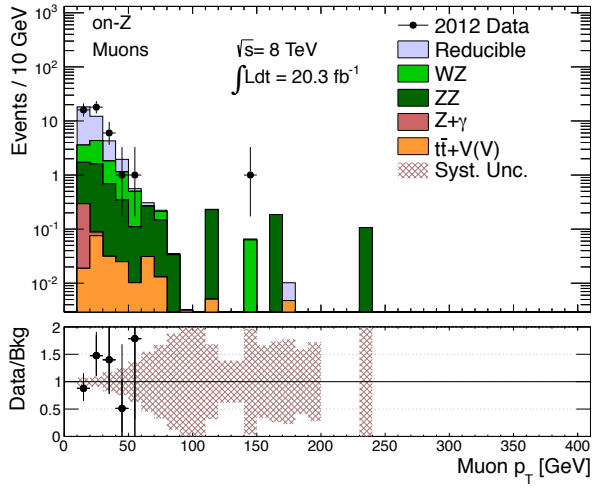

(c) Intermediate muon p_{T}

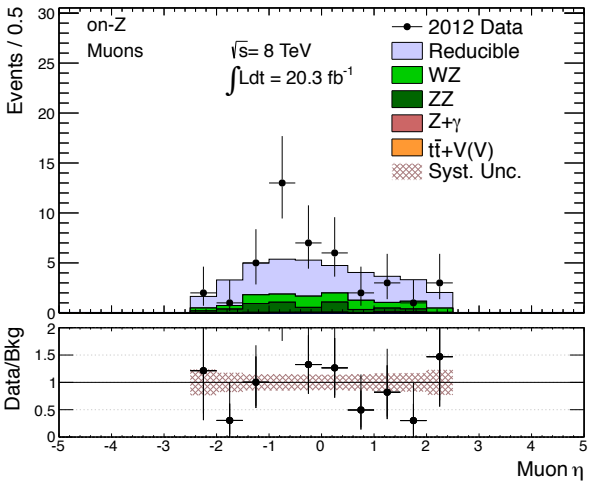

(d) Intermediate muon η

Figure 7.5: p_{T} and η distributions of the off-Z electron (top) or muon (bottom) satisfying the intermediate selection criteria. The other two leptons in the event are required to satisfy the numerator selection criteria and form an opposite-sign, same-flavor pair, with different flavor from the intermediate lepton.

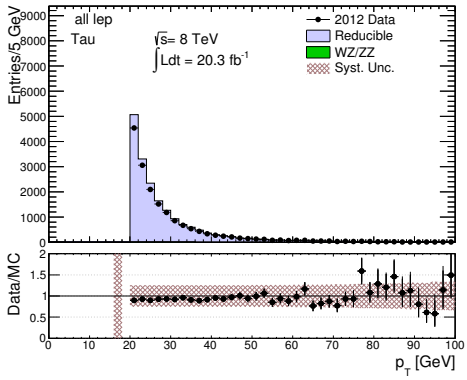

(a) Intermediate τ_{had} p_T, on-Z

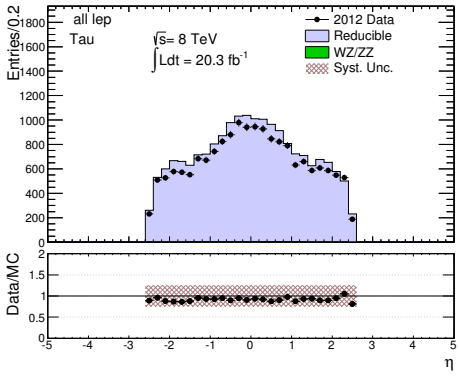

(b) Intermediate τ_{had} η, on-Z

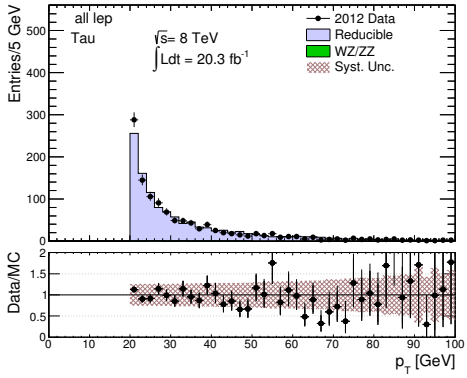

(c) Intermediate τ_{had} p_T, off-Z/OSSF

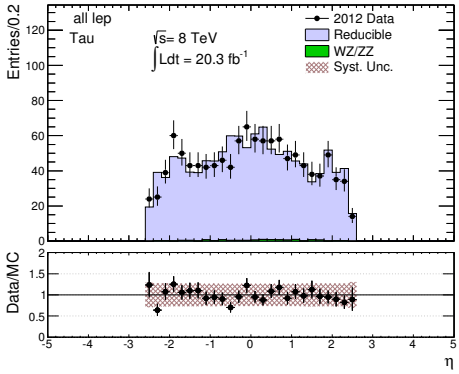

(d) Intermediate τ_{had} η, off-Z/OSSF

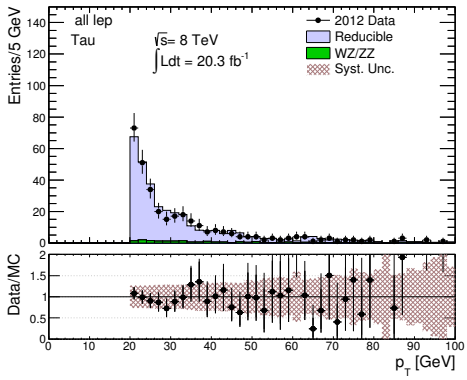

(e) Intermediate τ_{had} p_T, off-Z/mixed

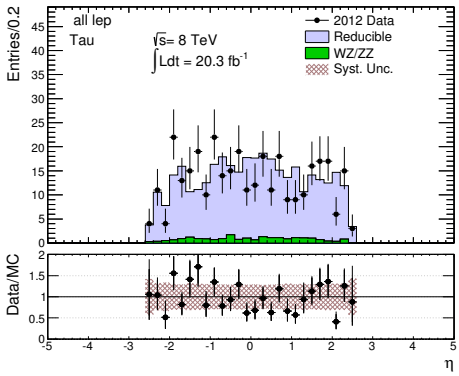

(f) Intermediate τ_{had} η, off-Z/mixed

Figure 7.6: p_{T} and η distributions of the intermediate τ_{had} in the on-Z, off-Z/OSSF, and off-Z/mixed intermediate validation regions.

7.5 Results and Limits

The results of the search as organized as follows. For each category, the distributions of the various kinematic variables ($H_{\mathrm{T}}^{\mathrm{leptons}}$, $H_{\mathrm{T}}^{\mathrm{jets}}$, m_{eff}, $E_{\mathrm{T}}^{\mathrm{miss}}$, m_{T}^{W}, N_{jets}, $N_{b-\mathrm{tags}}$, and the p_{T} of the third lepton) are produced (where applicable). Then, in each of the 138 signal regions, the number of observed and expected events are compared, and, absent any significant deviations, 95% confidence level (CL) upper limits are derived on the number of events from new physics, N_{95}, and the corresponding *visible cross section*, $\sigma_{95}^{\mathrm{vis}}$, defined as

$$\sigma_{95}^{\mathrm{vis}} = \frac{N_{95}}{\mathcal{L}}, \tag{7.3}$$

where $\mathcal{L} = 20.3$ fb^{-1} is the integrated luminosity of the data.

The plots for the $H_{\mathrm{T}}^{\mathrm{leptons}}$ signal regions are shown here for demonstrative purposes. The full set of plots is available at [**model-independent-webpage**]. The $H_{\mathrm{T}}^{\mathrm{leptons}}$ distributions are shown in figure 7.7. The observed and expected event counts in the three corresponding signal regions ($H_{\mathrm{T}}^{\mathrm{leptons}} > 200$ GeV, $H_{\mathrm{T}}^{\mathrm{leptons}} > 500$ GeV, and $H_{\mathrm{T}}^{\mathrm{leptons}} > 800$ GeV) are shown in table 7.3. Finally, the upper limits on $\sigma_{95}^{\mathrm{vis}}$ are shown in figure 7.8.

The deviations between the observed and expected in all 138 signal regions are shown in figure 7.9, in units of the total uncertainty on the background expectation.

Figure 7.7: $H_{\mathrm{T}}^{\mathrm{leptons}}$ distributions in the six categories.

Table 7.3: Observed and expected event counts in the $H_{\mathrm{T}}^{\mathrm{leptons}}$ signal regions, along with the inclusive counts for the entire category.

7.6 Model Testing

The 95% CL upper limits on trilepton event production from new physics derived in section 7.5 provide a useful tool with which to confront models of new physics producing trilepton final states. To facilitate the comparison of the model-independent limits with the

Figure 7.8: 95% CL upper limits on the visible cross section of trilepton event production from new physics, $\sigma_{95}^{\mathrm{vis}}$, in each $H_{\mathrm{T}}^{\mathrm{leptons}}$ signal region.

Figure 7.9: Deviations between the observed event counts and the background expectations in each signal region, in units of the total uncertainty on the background prediction.

predictions of a model (i.e. a set of simulated events from an event generator), per-lepton fiducial efficiencies are provided to quantify approximately the efficiency of triggering, reconstructing and selecting fiducial leptons at truth level. The definition of fiducial truth leptons is as follows:

- **Transverse momentum**: Electrons and muons are required to have $p_{\mathrm{T}} > 10$ GeV, while tau leptons are required to have $p_{\mathrm{T}} > 15$ GeV.
- **Pseudorapidity**: The same pseudorapidity cuts as the reconstructed signal leptons are applied. Electrons must have $|\eta| < 2.47$, excluding the region $1.37 < |\eta| < 1.52$, and muons and tau leptons must have $|\eta| < 2.5$.
- **Isolation**: For electrons and muons, the sum of the transverse momenta of all charged particles with $p_{\mathrm{T}} > 1$ GeV within a cone of radius $\Delta R = 0.3$ of the lepton, denoted `truth_ptcone30`, must satisfy `truth_ptcone30`$/p_{\mathrm{T}} < 0.15$. Similarly, the `truth_Etcone30`, defined as the sum of all stable, visible particles within a cone of radius $\Delta R = 0.3$, is required to satisfy `truth_Etcone30`$/p_{\mathrm{T}} < 0.15$.
- **Origin and Decay**: Leptons must originate from the hard scattering interaction (as opposed to the interaction with the detector as simulated by GEANT4), and not arise from the decay of a hadron. Electrons and muons are also required to be stable; tau leptons are required to decay hadronically.

The per-lepton fiducial efficiencies are measured in a sample of simulated WZ events. The efficiencies are determined separately for electrons, muons, hadronically decaying taus, electrons from tau decays, and muons from tau decays. Fiducial leptons are matched to reconstructed leptons satisfying the selection criteria (section 5.7.1), within a cone of $\Delta R = 0.1$ for electrons and muons and $\Delta R = 0.2$ for hadronically decaying taus and electrons and muons from τ decays. The efficiency, ϵ_ℓ, is the ratio of the number of matched reconstructed leptons to the number of fiducial leptons within the geometrical acceptance. For electrons, hadronically decaying taus, and electrons from tau decays, the efficiency is measured separately in bins of p_{T} and $|\eta|$, with the efficiency of a given lepton taken to be $\epsilon_\ell(p_{\mathrm{T}}, \eta) \equiv \epsilon_\ell(p_{\mathrm{T}}) \cdot \epsilon_\ell(|\eta|)/\langle\epsilon_\ell\rangle$, where $\langle\epsilon_\ell\rangle$ is the average efficiency of the inclusive sample. For muons, the efficiency is measured in bins of p_{T} for $|\eta| < 0.1$ and $|\eta| > 0.1$.

The efficiencies are shown in tables 7.4 and 7.5. Given a model of new physics, they can be used to compute the number of events expected in each of the signal regions; for example, an event with three leptons ℓ_1, ℓ_2, and ℓ_3 has an efficiency $\epsilon = \epsilon_{\ell_1}\epsilon_{\ell_2}\epsilon_{\ell_3}$ to be reconstructed and selected.

7.6.1 Example: Doubly Charged Scalar Particles

An an example of confronting models of new physics with the model-independent limits in section 7.5, limits are established on a model of predicting doubly charged scalar particles

p_{T}	Prompt e	Prompt μ		$\tau \to e$	$\tau \to \mu$		τ_{had}
[GeV]		$\lvert\eta\rvert > 0.1$	$\lvert\eta\rvert < 0.1$		$\lvert\eta\rvert > 0.1$	$\lvert\eta\rvert < 0.1$	
10–15	0.045±0.001	0.021±0.001	0.003±0.002	0.027±0.002	0.013±0.001	0.005±0.003	-
15–20	0.484±0.003	0.704±0.003	0.37±0.01	0.384±0.005	0.539±0.005	0.29±0.02	0.071±0.003
20–25	0.571±0.003	0.808±0.002	0.42±0.01	0.47±0.01	0.62±0.01	0.35±0.03	0.25±0.01
25–30	0.628±0.002	0.855±0.002	0.45±0.01	0.52±0.01	0.68±0.01	0.39±0.03	0.31±0.01
30–40	0.681±0.002	0.896±0.001	0.50±0.01	0.57±0.01	0.71±0.01	0.42±0.03	0.31±0.01
40–50	0.713±0.002	0.920±0.001	0.52±0.01	0.60±0.01	0.75±0.01	0.42±0.04	0.31±0.01
50–60	0.746±0.002	0.932±0.001	0.52±0.01	0.64±0.01	0.76±0.01	0.42±0.03	0.31±0.01
60–80	0.767±0.002	0.940±0.001	0.52±0.01	0.67±0.01	0.78±0.01	0.42±0.03	0.32±0.01
80–100	0.800±0.003	0.940±0.002	0.52±0.01	0.68±0.02	0.79±0.02	0.42±0.04	0.32±0.02
100–200	0.820±0.003	0.940±0.002	0.52±0.01	0.70±0.03	0.81±0.02	0.42±0.05	0.32±0.02
200–400	0.83±0.01	0.94±0.01	0.52±0.05	0.72±0.08	0.91±0.06		0.29±0.05
400–600	0.83±0.04	0.93±0.02	0.50±0.20				
≥ 600	0.83±0.05	0.92±0.08					

Table 7.4: The fiducial efficiency for electrons, muons, and taus in different p_{T} ranges ($\epsilon_{fid}(p_{\mathrm{T}})$). For electrons and muons from tau decays, the p_{T} is that of the electron or muon, not the tau. The uncertainties shown reflect the statistical uncertainties of the simulated samples only.

$\lvert\eta\rvert$	Prompt e	$\tau \to e$	τ_{had}
0.0–0.1	0.640±0.003	0.37±0.01	0.24±0.01
0.1–0.5	0.699±0.001	0.41±0.01	0.31±0.01
0.5–1.0	0.702±0.001	0.41±0.01	0.28±0.01
1.0–1.5	0.660±0.002	0.37±0.01	0.21±0.01
1.5–2.0	0.605±0.002	0.36±0.01	0.25±0.01
2.0–2.5	0.602±0.002	0.38±0.01	0.25±0.01

Table 7.5: The fiducial efficiency for electrons and taus in different η ranges ($\epsilon_{fid}(\eta)$). For electrons from tau decays, the η is that of the electron, not the tau. The uncertainties shown reflect the statistical uncertainties of the simulated samples only.

within the context of left-right symmetry [5–8]. The model contains several scalar particles of charge 0, ±1, and ±2, the neutral component of which generates neutrino mass via the seesaw mechanism (section 2.2.3). Only pair production of the doubly charged particles, $H^{\pm\pm}_{L,R}$, is considered here, where L denotes coupling to $\mathrm{SU}(2)_L$ or $\mathrm{SU}(2)_R$. The phenomenology of the particles is similar, differing in their couplings to left- and right-handed fermions and in their pair production cross sections due to different gauge couplings.

The $H^{\pm\pm}_{L,R}$ decay to two charged leptons, and in general do not conserve lepton flavor. In scenarios where the $H^{\pm\pm}_{L,R}$ decay to electrons or muons, the strongest limits are derived from same-sign dilepton signatures. An ATLAS search at $\sqrt{s} = 8\,\mathrm{TeV}$ excluded $H^{\pm\pm}_L$ masses below $465\,\mathrm{GeV} - 550\,\mathrm{GeV}$ and $H^{\pm\pm}_R$ masses below $370\,\mathrm{GeV} - 435\,\mathrm{GeV}$, depending on the flavor of the lepton pair ($e^\pm e^\pm$, $e^\pm\mu^\pm$, or $\mu^\pm\mu^\pm$) [9]. If the $H^{\pm\pm}_{L,R}$ decay to $e^\pm\tau^\pm$ or $\mu^\pm\tau^\pm$, however, then competitive limits can be established using model-independent trilepton limits.

The model is confronted against the model-independent limits in the off-Z, OSSF categories, using the $H_{\mathrm{T}}^{\mathrm{leptons}}$ signal regions and combining the **3L** and **2L**+τ_{had} categories. Events are simulated using PYTHIA8 using the MSTW2008 leading order PDF set, with mass hypotheses in 50 GeV increments between $50\,\mathrm{GeV} - 600\,\mathrm{GeV}$, plus an additional point at a mass of 1 TeV. The $H_{\mathrm{T}}^{\mathrm{leptons}} > 200\,\mathrm{GeV}$ signal regions are used for $H^{\pm\pm}$ mass hypotheses below 200 GeV, while the $H_{\mathrm{T}}^{\mathrm{leptons}} > 500\,\mathrm{GeV}$ signal regions are used for larger mass hypotheses. The resulting observed and expected limits are shown in figure 7.10. For left-handed doubly charged particles, masses below 400 GeV (400 GeV) are excluded for 100% branching fraction to $e^\pm\tau^\pm$ ($\mu^\pm\tau^\pm$), compared to expected limits of $350 \pm 50\,\mathrm{GeV}$ ($370 \pm 20\,\mathrm{GeV}$).

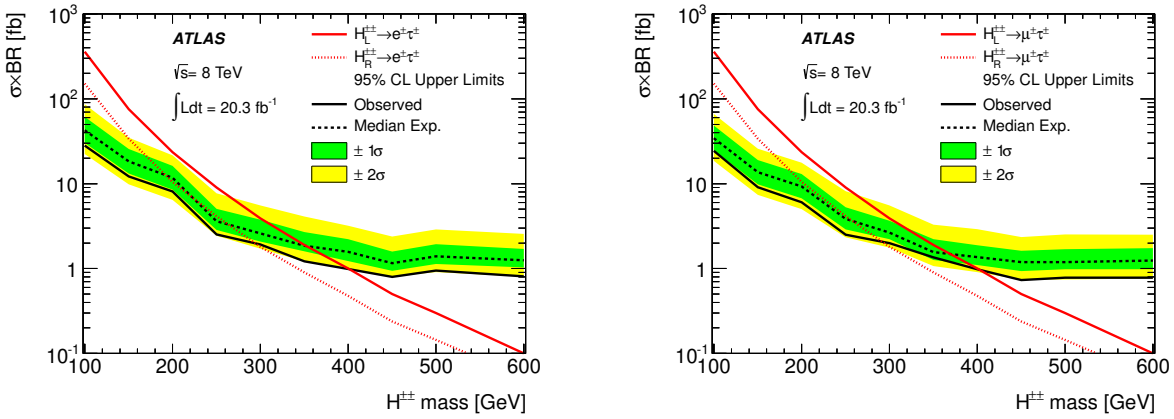

(a) $H^{\pm\pm} \to e^\pm\tau^\pm$ (b) $H^{\pm\pm} \to \mu^\pm\tau^\pm$

Figure 7.10: Observed and expected 95% CL limits on the cross section times branching ratio for $H^{\pm\pm}$ decaying to $e^\pm\tau^\pm$ (left) and $\mu^\pm\tau^\pm$ (right). The solid and dashed red lines show the expected cross section times branching ratio for left- and right-handed $H^{\pm\pm}$, respectively.

Bibliography

[1] The ATLAS Collaboration, *Search for new phenomena in events with three or more charged leptons in pp collisions at $\sqrt{s} = 8$ TeV with the ATLAS detector*, arXiv.org (Nov. 2014), arXiv: 1411.2921v2 [hep-ex], URL: http://arxiv.org/abs/1411.2921v2.

[2] The ATLAS Collaboration, *Jet energy measurement and its systematic uncertainty in proton–proton collisions at $\sqrt{s} = 7$ TeV with the ATLAS detector*, English, The European Physical Journal C **75**.1 (Jan. 2015) pp. 17–101, URL: http://link.springer.com/10.1140/epjc/s10052-014-3190-y.

[3] M. V. Garzelli et al., *Z^0-boson production in association with a $t\bar{t}$ pair at next-to-leading order accuracy with parton shower effects*, English, Physical Review D **85**.7 (Apr. 2012) pp. 074022–6, URL: http://link.aps.org/doi/10.1103/PhysRevD.85.074022.

[4] J. M. Campbell and R. K. Ellis, *$t\bar{t}W^{\pm}$ production and decay at NLO*, English, JHEP **2012**.7 (July 2012) pp. 52–12, URL: http://link.springer.com/10.1007/JHEP07(2012)052.

[5] J. C. Pati and A. Salam, *Lepton Number as the Fourth Color*, Phys.Rev. **D10** (1974) pp. 275–289.

[6] R. N. Mohapatra and J. C. Pati, *Left-Right Gauge Symmetry and an Isoconjugate Model of CP Violation*, English, Phys.Rev. **D11**.3 (1975) pp. 566–571, URL: http://link.aps.org/doi/10.1103/PhysRevD.11.566.

[7] G. Senjanovic and R. N. Mohapatra, *Exact Left-Right Symmetry and Spontaneous Violation of Parity*, English, Phys.Rev. **D12**.5 (1975) pp. 1502–1505, URL: http://link.aps.org/doi/10.1103/PhysRevD.12.1502.

[8] T. G. Rizzo, *Doubly Charged Higgs Bosons and Lepton Number Violating Processes*, Phys.Rev. **D25** (1982) pp. 1355–1364.

[9] *Search for anomalous production of prompt same-sign lepton pairs and pair-produced doubly charged Higgs bosons with $\sqrt{s} = 8$ TeV pp collisions using the ATLAS detector*, English, **2015**.3 (Mar. 2015) pp. 41–48,
URL: http://link.springer.com/article/10.1007/JHEP03(2015)041.